Gallien, Anthony; Prawda, Karolina; Schlecht, Sebastian J.

Matching early reflections of simulated and measured RIRs by applying sound-source directivity filters

Published in:
4th International Conference on Acoustics and Sound Reinforcement, ASR 2024

Published: 01/01/2024

Document Version
Publisher's PDF, also known as Version of record

Audio Engineering Society

Conference Paper 1

Presented at the International Conference on Acoustics & Sound Reinforcement
2024 January 22–26, Le Mans, France

Matching early reflections of simulated and measured RIRs by applying sound-source directivity filters

Anthony Gallien[1], Karolina Prawda[2], and Sebastian J. Schlecht[2,3]

[1] *ENSEA, Cergy, France*
[2] *Acoustics Lab, Dept. Inofrmation and Communications Engineering, Aalto University, Espoo, Finland*
[2] *Media Lab, Dept. Art and Media, Aalto University, Espoo, Finland*

Correspondence should be addressed to Anthony Gallien (anthony.gallien12@gmail.com)

ABSTRACT

Acoustic measurements are susceptible to various sources of measurement uncertainty. One significant factor is loudspeaker directivity, which introduces temporal smearing and spectral coloration into room impulse responses (RIRs), predominantly influencing early reflections. Such an artifact affects parametric processing and perceptual evaluation of RIRs and lowers the measurement reproducibility. This study evaluates the impact of loudspeaker directivity on measured RIRs. We acquire directivity filters via measurements in an anechoic chamber, utilizing a custom-made microphone arc. Subsequently, we both capture a series of RIRs in a typical reverberant room and simulate corresponding RIRs with the image-source method (ISM). By convolving the simulations with the correct directivity filters, we match the early reflections of measured and simulated RIRs. Examining the cross-correlation between the simulated and measured RIRs reveals a pronounced likeness for first-order reflections, indicating a substantial influence of the loudspeaker directivity on recorded RIRs. This study is a step towards accounting for the influence of the sound source type and position on RIRs, resulting in better-informed acoustic measurements and higher fidelity of acoustic simulations.

1 Introduction

Room impulse response (RIR) measurements are burdened by uncertainty originating from several sources [1, 2]. One of them is the loudspeaker directivity [3, 4, 5, 6], which is present even in the dodecahedral and spherical sound sources conforming with the ISO standard regarding omnidirectivity [4, 7].

The sound-source directivity introduces temporal smearing (i.e., distortion of the transient nature of the reflections) and spectral coloration to the recorded signal. The effects are visible, especially in the early part of the RIR, i.e., direct sound and early reflections, where the pulses are still relatively well separated [4]. The unwanted consequences of sound-source directivity affect the estimation of the acoustic parameters [3, 4] and lower the measurement reproducibility, as well as influence parametric processing and perceptual evaluation of audio. In the present study, we evaluate the extent of this effect by assessing the directivity of multiple sound sources typically used in RIR measurements and sound reproduction.

Inaccurate modeling of sound-source properties is one reason behind discrepancies between measured and simulated RIRs [8, 9, 10]. Despite this, conventional RIR simulation tools, such as the image-source method (ISM), often overlook the sound-source directivity in their implementation [11, 12]. This study assesses how much similarity between measured and synthesized RIRs is lost due to the point-source assumption.

This work evaluates the influence of loudspeaker directivity on the early reflections of RIRs. We start by measuring the directivity filters of several sound sources in an anechoic chamber. We use the same equipment to collect RIRs in a typical shoebox room. We then select the directivity filters corresponding to first-order reflections by using the ISM to derive the departure direction of reflections. The comparison between measured RIRs and ISM-modeled ones convolved with directivity filters shows the amount of directivity-induced filtering in measured RIRs.

The paper is organized as follows. Sec. 2 describes the equipment and procedure for gathering the loudspeaker directivity filters. Sec. 3 elaborates on the RIR measurements. The results of matching the measured and simulated RIRs are presented in Sec. 4. Sec. 5 summarizes and concludes the paper.

2 Directivity filters

The first step of this research is to acquire a set of directivity filters for a diverse set of loudspeakers.

Loudspeaker directivity measurements, also those done by loudspeaker manufacturers [13], are usually conducted in an anechoic chamber [8], where a loudspeaker is rotated using a turntable. Typically, a single microphone records one IR for different azimuth angles. However, this method has the disadvantage of only recording the loudspeaker directivity along the horizontal plane. Alternatively, placing the loudspeaker on its side can result in the directivity of the vertical plane. The measurement resolution can be further increased by placing either the loudspeaker of a microphone on a swivel arm [8].

Our study, which focuses on three-dimensional (3D) sound propagation, requires directivity filters for the entire sphere surrounding the loudspeaker rather than only focusing on the horizontal or vertical axis. Thus, a measurement of the directivity along the Z-axis was necessary for every rotation angle in the horizontal plane.

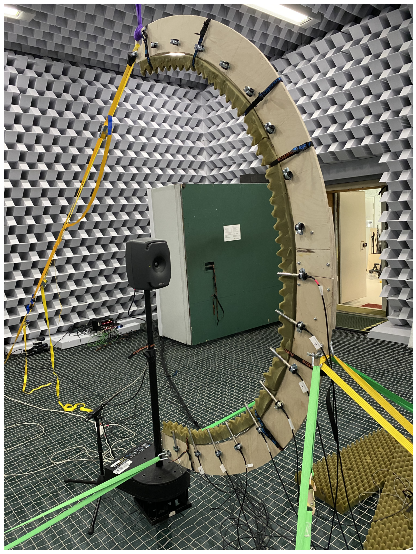

Fig. 1: Directivity filters measurement setup with the microphone holder and GENELEC 8331A loudspeaker.

2.1 Measurement arc

To secure high resolution of directivity characteristics over 180° of elevation angle, we built a concentric semicircular microphone array with a radius of one meter, inspired by the measurement arc developed by Meyer-Kahlen *et al.* [14]. The measurement arc used in this study is presented in Fig. 1.

The structure is built from plywood parts, to which microphones are attached with hose clamps. The distance between the measured sound source and the sound receivers is 1 m. To ensure the least amount of reflections during the measurement, the plywood parts facing the direction of the loudspeaker were only 15 mm thick. An additional layer of acoustic foam further decreases its reflective properties.

The microphone positions on the arc span 170°, from $-80°$ to 90° w.r.t. the horizontal plane. The angular step is 10°, amounting to a total of 18 microphone positions.

2.2 Measurement procedure

Fig. 1 depicts the setup used in the directivity measurements. The procedure was conducted in an anechoic

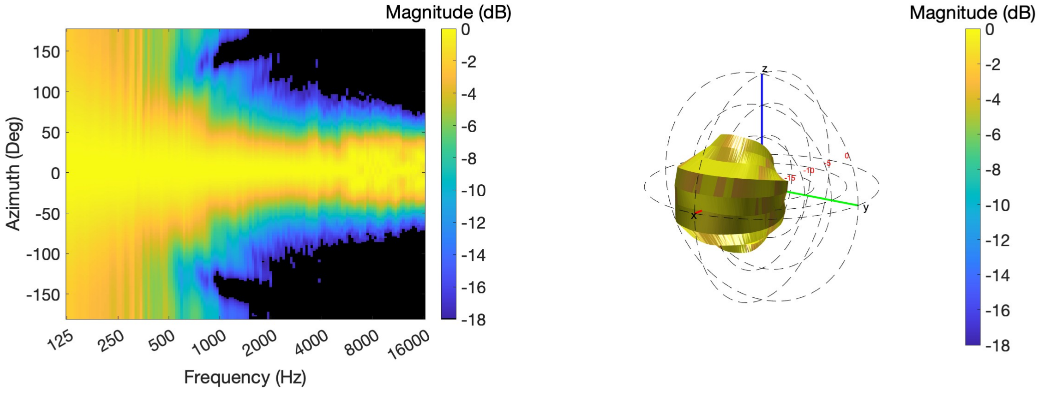

(a) (b)

Fig. 2: GENELEC 8331A directivity (a) horizontal plane (microphone at 0° elevation) (b) whole sphere at 6 kHz.

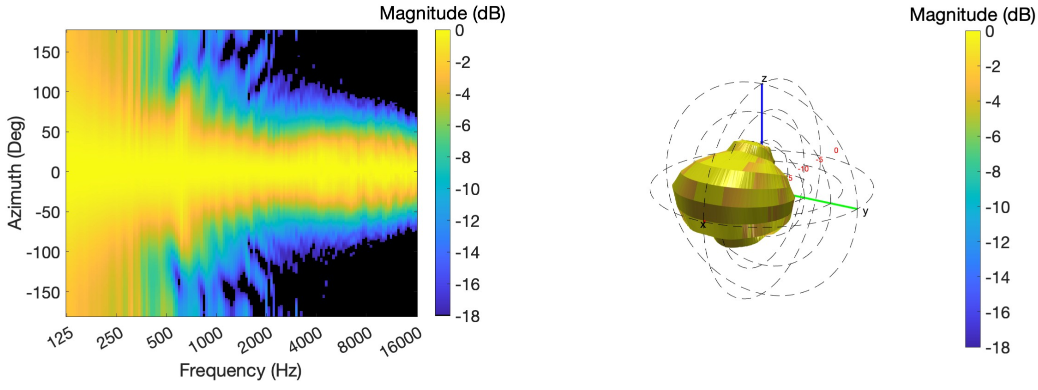

(a) (b)

Fig. 3: GENELEC 8030B directivity (a) horizontal plane (microphone at 0° elevation) (b) whole sphere at 6 kHz.

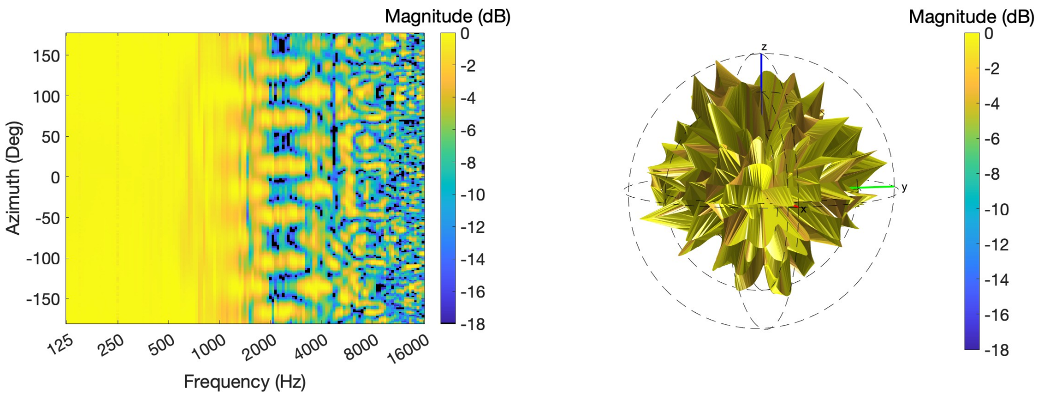

(a) (b)

Fig. 4: Omni-source directivity (a) horizontal plane (microphone at 0° elevation) (b) whole sphere at 6 kHz.

chamber, a facility of Aalto University's Acoustics Lab in Espoo, Finland. The chamber has dimensions of 8.2 m×8.2 m×7.2 m (length, width, and height, respectively) and is anechoic for frequencies over 50 Hz. Evaluated loudspeakers were placed on a stand attached to a turntable with a 1-degree rotation resolution in the horizontal plane.

The measurement signal was an exponential sine-sweep [15] sampled at 48 kHz, played for every turntable angle, and simultaneously recorded by all microphones. The RIRs were obtained by deconvolution using the inverse sweep. Thus, we obtained $360 \times 18 = 6480$ directivity filters for each loudspeaker corresponding to every turntable and measurement arc angle combination. The complete data set was saved in the Spatially Oriented Format for Acoustics (SOFA) [16].

We used eight G.R.A.S. 1/2" free-field microphones of type 46AF and one Brüel & Kjær 1/2" free-field microphone of type 4191 powered by a G.R.A.S type 12AG and a G.R.A.S type 12HF power modules. The calibration was applied in the post-processing on the collected directivity filters. All the measurements were adjusted so that their magnitudes were equal around 30 Hz, where the loudspkeaer is assumed to be a point source, meaning that the direction did not affect the magnitude value.

To minimize the risk of non-stationary noise influencing the measurements, we repeated each measurement twice and examined the correlation coefficient of each pair [17]. The temperature in the room was recorded as well, and the procedure started no sooner than six minutes after the last person left the room, lowering the effect of time variance on the results [7]. The microphone holder was laser-positioned.

Three different loudspeakers were evaluated in the procedure: two directional studio loudspeakers, GENELEC 8331A (shown in Fig. 1), GENELEC 8030B, and one omnidirectional loudspeaker, 01dB LS01 sound source. The measured directivity patterns are depicted in Fig. 2, Fig. 3, and Fig. 4 in two ways: on the horizontal plane (for the elevation angle of 0°) over the entire frequency range and a spherical pattern for one frequency band (in this case 6 kHz).

The figures show that both studio loudspeakers display directional properties above 400 Hz, with a strong directional pattern appearing above $1-2$ kHz. The energy radiated by the omni-source is much more even, with strong fluctuation occurring above 1.5 kHz. The complete directivity measurement database and the results are available online[1].

3 RIR Measurements

This section describes the measurement procedure for capturing RIRs in a reverberant shoebox room. We also explain the method of determining the most optimal source-receiver positions to visualize the influence of the loudspeaker directivity.

3.1 Positions determination

During the measurements in the reverberant room, we obtained RIRs with the maximum possible temporal separation of reflections in the early part (i.e., the direct sound and early reflections) of the signal. We aimed for the maximal number of reflections that did not overlap. This allowed for a reliable estimation of the departure directions from the loudspeaker. Thus, directivity filters that corresponded with the early reflections of the RIR could be readily chosen (*cf.* Sec. 4.1). The proposed method applies equally well to other source-receiver positions, but the effect is less easily visualized in the time domain.

We synthesized up to second-order reflections using ISM to determine the source and receiver positions. First, we chose the loudspeaker position as the center of the room $[x,\ y,\ z] = [3.6,\ 2.75,\ 1.1]$ m. We opted for two different microphone heights: 1.5 m and 2 m. To identify the optimal microphone position, where the time separation between two reflections was maximized, we performed ISM simulations for every x- and y-position, corresponding to a specific microphone height and source position. Because of the symmetries of the room, we varied the x-position from 0.1 m to 2.6 m and the y-position from 0.1 m to 5.4 m with a step size of 0.1 m.

The example simulation results for $z = 2$ m are presented in Fig. 5(a). The tested measurement positions are marked in the evaluated area of the room, with shades of gray indicating the minimal time interval between consecutive reflections. The dark regions suggest good candidate positions for microphone placement, where the recorded reflections did not overlap in time.

[1] `http://research.spa.aalto.fi/publications/papers/aes-asr24-recreate-RIRs/`

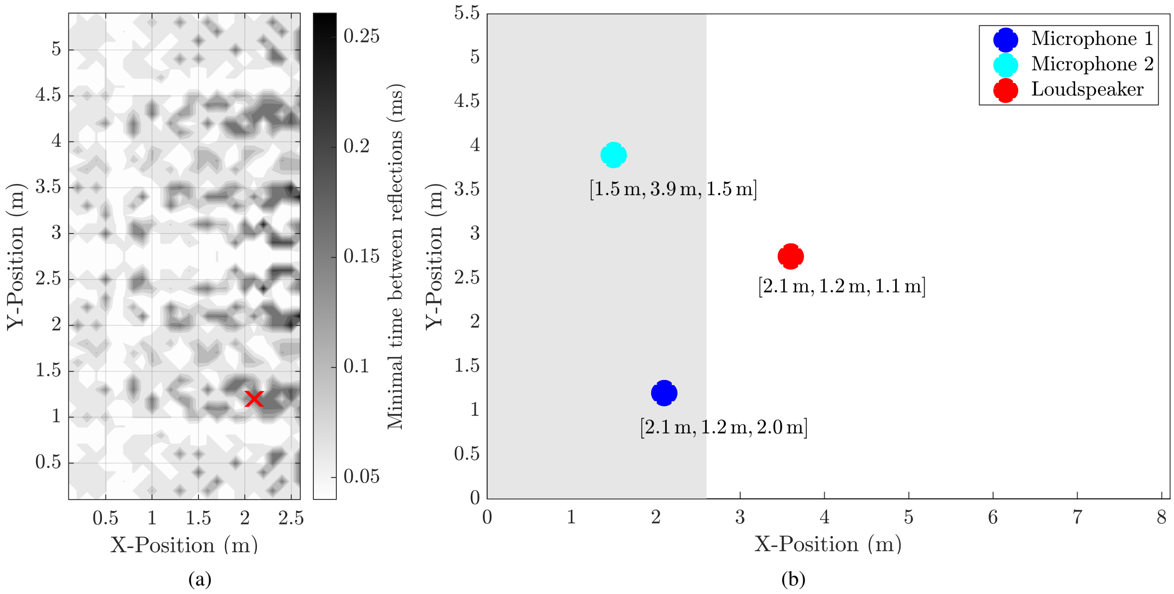

Fig. 5: Measurement Positions: (a) Simulation to determine the best microphone position for a height of 2 m. The red *X* marks the placement selected for the measurements. (b) Loudspeaker and microphone positions during the RIR measurements. The shaded region corresponds to the area evaluated for microphone placement in (a). The microphone 1 position (blue dot) corresponds to the maximum found in (a) indicated by the red *X* mark.

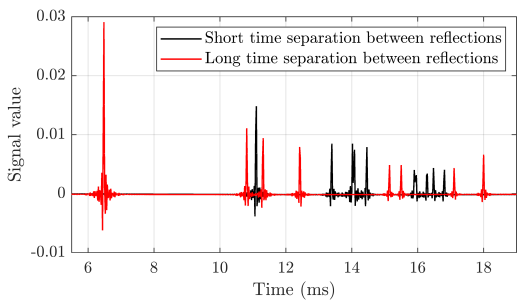

Fig. 6: ISM-simulated RIRs of the reverberant room showing the microphone positions for which time separation between reflection is short (*c.f.* white areas in Fig. 5(a)) and long (*c.f.* dark areas in Fig. 5(a)).

The difference in time separation of reflections for a microphone position in white and dark areas of Fig. 5(a) is depicted in Fig. 6. To prevent simultaneous reflections, we deliberately avoided placing the microphones on the room's axes of symmetry.

Consequently, for the microphone placed at $z = 2$ m, we choose the coordinates $[x, y] = [2.1, 1.2]$ m as illustrated in Fig. 5(a). Fig. 5(b) depicts the positions chosen for the two microphones due to the ISM simulations. It also shows the area that was considered in microphone position determination.

3.2 Measurement setup

The RIRs were collected in a variable acoustics room *Arni* at the Aalto University Acoustics Lab. It is a shoebox room of size 8.1 m×5.5 m×3.2 m (length, width, and height, respectively). The measurements were conducted in the most reverberant setting to ensure the maximum amount of clear reflections when all the acoustic panels on the walls and ceiling were closed [18, 19].

The excitation signal was a 3-second sweep, with frequencies spanning 20 Hz to 20 kHz. We used two G.R.A.S. 1/2" free-field microphones as sound receivers and all loudspeakers described in Sec. 2 as sound sources. The measurement setups for each loudspeaker are depicted in Fig. 7. As we used only the direct sound and early reflections in further analysis, the signal-to-noise ratio obtained with a single sweep was sufficient.

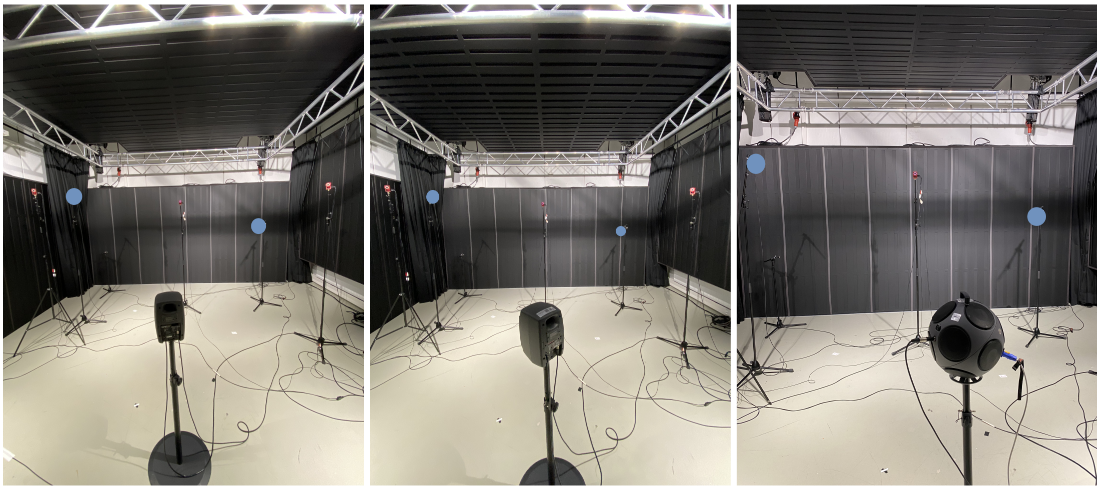

(a) (b) (c)

Fig. 7: RIR Measurement setup in *Arni* using (a) GENELEC 8030B (b) GENELEC 8331A (c) Omni-source. The microphone positions are marked with blue dots. N.B. different camera angles in each photo.

4 Results

In the following, we present the results of RIR matching between ISM simulations and measurements. We estimate the correct directivity filters based on the departure direction of reflections using ISM. We then compare the results of the proposed method to using plain ISM and random directivity filters in the matched RIRs.

4.1 RIR simulation

We used ISM simulations of the room with the same sound source and receiver positions as during the measurements to estimate the departure direction of reflections and applied the corresponding directivity filters. We used the first- and second-order reflections only, as they belong to the early part of the RIR and are well separated from each other.

We estimated the image-source positions and traced the sound paths from the receiver to each source, as depicted in Fig. 8. We used the path lengths to compute the time delay of each reflection, thus assigning a correct image source to each reflection in the RIR. In the calculations, we used the speed of sound in 20° C and dry air, 343 m/s. However, the choice of this value is only heuristic, as later on, the time-of-arrival of reflections was manually adjusted to fit the measurements.

Using the traced sound paths, we determined the reflections' azimuth and elevation angles according to the schematics depicted in Fig. 9. In each of the measurements, the loudspeaker's vertical axis was aligned with the microphone position, setting the azimuth of the direct sound to 0°. Consequently, the azimuth angles of the remaining reflections were established relative to the direct path. The elevation was expressed relatively to the horizontal (XY) plane. Fig. 10 presents the estimated values of the angles for every reflection. They correspond to the angles of the measured directivity filters.

4.2 RIR matching

To match the ISM-simulated RIRs with the measured ones, we manually adjusted the time of ISM reflections to fit the measurements. We also matched the reflections' peak value to simulate energy losses due to surface and air absorption. To accurately evaluate the influence of directivity filters on RIR similarity, we compared three approaches: using plain ISM, using random directivity filters, i.e., without considering the departure direction, and the directivity filters corresponding to the estimated departure direction.

The examples of matched RIRs are presented in Fig. 11(a), Fig. 11(b), and Fig. 11(c). In Fig. 11(a), the plain ISM simulation does not capture the details of

Loudspeaker	GENELEC 8331A		GENELEC 8030B		Omni-Source	
Microphone	1	2	1	2	1	2
Correct filters	0.81	0.80	0.59	0.67	0.36	0.42
Random filters	0.52	0.46	0.35	0.30	0.28	0.23
ISM Simulation	-0.70	-0.71	-0.03	0.28	-0.29	-0.30

Table 1: Correlation coefficients between measurements and different signals for the first five reflections.

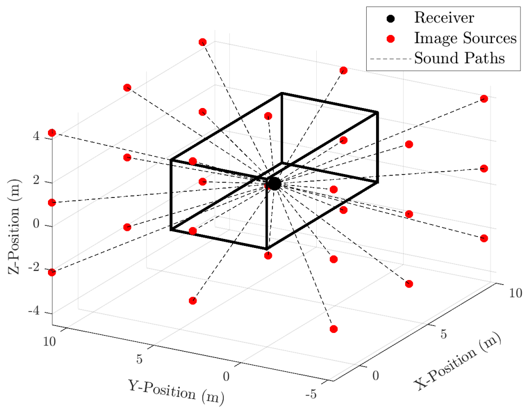

Fig. 8: Image-source positions and sound paths between sources and the receiver used for estimating the departure direction.

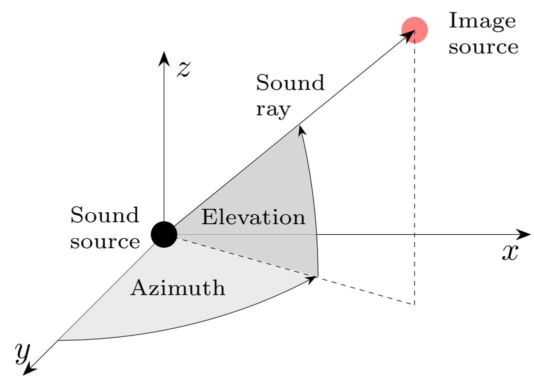

Fig. 9: The azimuth and elevation angles with respect to the sound source and the coordinate system.

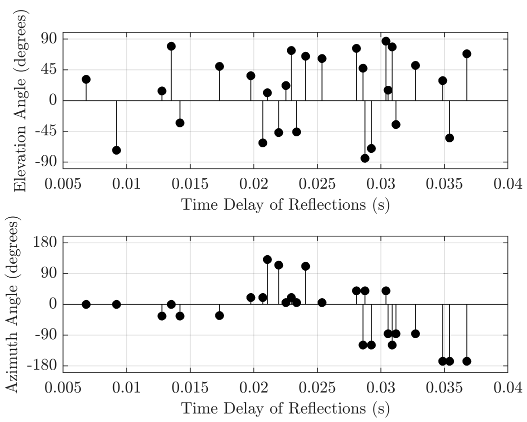

Fig. 10: The elevation and azimuth angles of the correct directivity filters are estimated from ISM simulations.

the temporal smearing and does not consider the phase of reflections, a common drawback of this technique [12]. Using directivity filters without considering the reflections' departure direction indicates the presence of temporal smearing; see Fig. 11(b). However, the shape of the reflections, the amount of smearing, and the phase information are incorrect most of the time. Using directivity filters respective to the correct departure direction shows the biggest similarity between measured and matched RIRs, although differences in reflections' shape are still visible and increase over time, see Fig. 11(c).

We estimated the cross-correlation between simulated and measured signals to evaluate the performance of the three RIR matching techniques. Table 1 shows the correlation coefficients determined for each sound source type and two microphone positions.

The highest similarity was obtained among all combinations when the correct directivity filters were used. Picking random filters lowered the correlation coefficient by $0.25-0.37$ for the studio loudspeakers, while this effect was significantly less prominent for the omni-

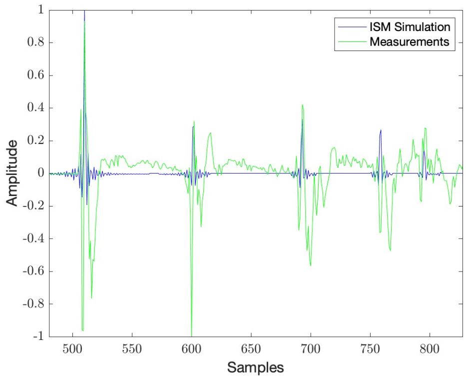

(a) RIR measurements and ISM Simulation for GENELEC 8030B and microphone 2.

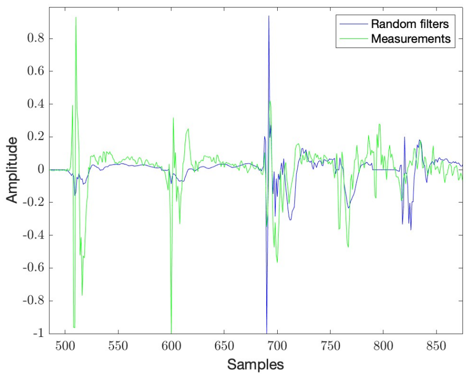

(b) RIR measurements and random filters for GENELEC 8030B and microphone 2.

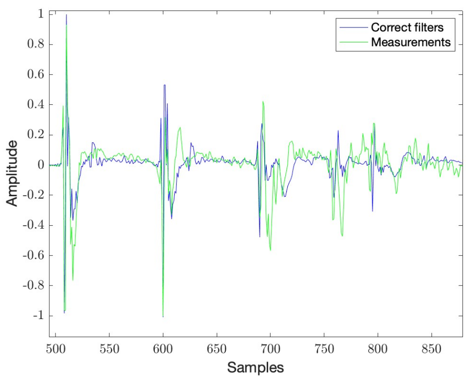

(c) RIR measurements and correct filters for GENELEC 8030B and microphone 2.

Fig. 11: Early time-domain room impulse response comparison.

source. This might be related to the directivity filters of the omnisource being generally similar to each other, while the filters of studio loudspeakers are significantly more dissimilar to each other. Applying no directivity filters in most cases resulted in a negative correlation coefficient, suggesting that the main factor for dissimilarity was the mismatched phase of reflections.

Table 1 shows that applying directivity filters to simulated RIRs had the biggest effect when using directional studio loudspeakers. The highest correlation coefficient values were obtained for the most directional GENELEC 8331A, while for the omni-source, it was most frequently close to zero. Such an effect might be explained by the omni-source outputting more energy in the high frequencies, which are more susceptible to atmospheric absorption and time variance in the measurement environment [20]. Consequently, matching the high-frequency content of reflections is harder than low frequencies, resulting in larger differences.

5 Conclusions

The paper addresses the issue of temporal smearing and spectral coloration in measured RIRs due to loudspeaker directivity. We first evaluated the directivity of three sound sources: two directional studio loudspeakers and an omnidirectional sound source commonly used in acoustic measurements. The obtained directivity filters created spherical directivity characteristics of each sound source.

The effect of sound-source directivity was evaluated on a set of RIRs measured in a typical shoebox room. Optimal receiver positions were estimated by examining the time separation between consecutive reflections simulated with ISM. Later, we used the ISM to estimate the departure direction of reflections from the loudspeaker to the microphone. After determining the correct directivity filters and applying them to early reflections of RIRs simulated via ISM, we obtain signals resembling the measured RIRs. We show that using the correct directivity filters increases the RIR similarity compared to utilizing plain ISM simulations or randomly chosen directivity filters.

The results of this study show that the loudspeaker directivity heavily affects the temporal properties of measured RIRs. Knowing the extent of this impact, the next step is to remove this influence to obtain RIRs impacted only by the room geometry, material properties, and propagation medium properties. The results presented in this study lead to better-informed acoustic measurements.

6 Acknowledgment

This work was conducted as Anthony Gallien's intership project at Aalto University Acoustics Lab from May 22 – August 18, 2023.

References

[1] Lundeby, A., Vigran, T. E., Bietz, H., and Vorländer, M., "Uncertainties of Measurements in Room Acoustics," *Acta Acust. un. Acust.*, 81(4), pp. 344–355, 1995.

[2] Witew, I. B. and Vorländer, M., "Influence of the exact source and receiver positions on the uncertainty of acoustical measurements in concert halls," *J. Acoust. Soc. Am.*, 141(5), pp. 3496–3496, 2017, doi:10.1121/1.4987309.

[3] Witew, I. B. and Behler, G. K., "Uncertainties in measurement of single number parameters in room acoustics," in *Proc. Forum Acusticum*, Budapest, Hungary, 2005.

[4] San Martín, R., Witew, I. B., Arana, M., and Vorländer, M., "Influence of the Source Orientation on the Measurement of Acoustic Parameters," *Acta Acust. un. Acust.*, 93(3), pp. 387–397, 2007.

[5] San Martín, R. and Arana, M., "Uncertainties caused by source directivity in room-acoustic investigations," *J. Acoust. Soc. Am.*, 123(6), pp. EL133–EL138, 2008, doi:10.1121/1.2838252.

[6] Witew, I., Müller-Giebeler, M., and Vorländer, M., "Evaluation and improvement of a model to predict the measurement uncertainty due to the directivity of room acoustical sound sources," *Proc. Meet. Acoust.*, 21(1), p. 015004, 2014, doi: 10.1121/1.4895587.

[7] Knüttel, T., Witew, I. B., and Vorländer, M., "Influence of "omnidirectional" loudspeaker directivity on measured room impulse responses," *J. Acoust. Soc. Am.*, 134(5), pp. 3654–3662, 2013, doi:10.1121/1.4824334.

[8] Aretz, M., *Combined wave and ray based room acoustic simulations of small rooms : challenges and limitations on the way to realistic simulation results*, Ph.D. thesis, Institute of Technical Acoustics, RWTH Aachen University, 2012.

[9] Vorländer, M., "Computer simulations in room acoustics: Concepts and uncertainties," *J. Acous. Soc. Am.*, 133(3), pp. 1203–1213, 2013, doi:10.1121/1.4788978.

[10] Brinkmann, F., Aspöck, L., Ackermann, D., Lepa, S., Vorländer, M., and Weinzierl, S., "A round robin on room acoustical simulation and auralization," *J. Acoust. Soc. Am.*, 145(4), pp. 2746–2760, 2019, doi:10.1121/1.5096178.

[11] Habets, E. A. P., "Room Impulse Response Generator," Technical report, Technische Universiteit Eindhoven, 2006.

[12] Lehmann, E. A. and Johansson, A. M., "Prediction of energy decay in room impulse responses simulated with an image-source model," *J. Acous. Soc. Am.*, 124(1), pp. 269–277, 2008.

[13] Tylka, J. G., Sridhar, R., and Choueiri, E., "A database of loudspeaker polar radiation measurements," in *Proc. 139th AES Conv.*, 2015.

[14] Meyer-Kahlen, N., Zotter, F., and Pollack, K., "Design and measurement of first-order, horizontally beam-controlling loudspeaker cubes," in *Proc. 144th AES Conv.*, 2018.

[15] Farina, A., "Simultaneous measurement of impulse response and distortion with a swept-sine technique," in *Proc. Audio Eng. Soc. 108th Conv.*, Paris, France, 2000.

[16] Audio Engineering Society, "AES standard for file exchange—Spatial acoustic data file format," Technical report, 2022.

[17] Prawda, K., Schlecht, S. J., and Välimäki, V., "Robust selection of clean swept-sine measurements in non-stationary noise," *J. Acoust. Soc. Am.*, 151(3), pp. 2117–2126, 2022, doi:doi.org/10.1121/10.0009915.

[18] Prawda, K., Schlecht, S. J., and Välimäki, V., "Evaluation of reverberation time models with variable acoustics," in *Proc. 17th SMC Conf.*, pp. 145–152, Torino, Italy, 2020.

[19] Prawda, K., Schlecht, S. J., and Välimäki, V., "Calibrating the Sabine and Eyring formulas," *J. Acoust. Soc. Am.*, 152(2), pp. 1158–1169, 2022, doi:10.1121/10.0013575.

[20] Prawda, K., Schlecht, S. J., and Välimäki, V., "Time Variance in Measured Room Impulse Responses," in *Proc. Forum Acusticum*, Turin, Italy, 2023.